



STELLAR MAGNETIC ACTIVITY (PAP351)

Lecture 4, February 7, 2024

Thomas Hackman



6. OBSERVING STARSPOTS

- The Sun can be studied by "direct" observations...
- ... but stars are typically too distant to be angularly resolved => inversion problems.
- Optical observations:
 - Photometry (usually UBV_R, or satellite filters)
 - Spectrometry
 - Spectropolarimetry
 - Interferometry



6.1 MAPPING STARSPOTS

- Three classes of methods to resolve stellar surfaces:
 - “Direct imaging”: But the objects are too distant.
 - Interferometry: May succeed for a small number of stars, but with poor resolution.
 - Inversion methods:
 - Doppler-imaging
 - Magnetic (“Zeeman”) Doppler-imaging
 - Photometric inversion
 - Exoplanetary transit mapping



6.1.1 DIRECT IMAGING OF A STELLAR SURFACE

- Diffraction limit for the angular resolution of a telescope:

$$\theta \sim \frac{\lambda}{D},$$

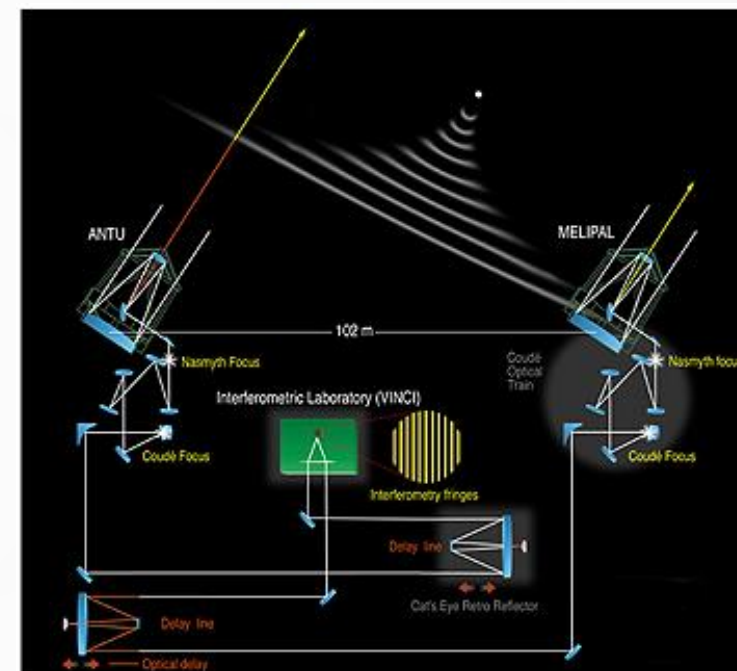
where D is the diameter of the telescope.

- Largest optical telescopes of the near future ~ 40 m, $\lambda \sim 6000 \text{ \AA}$
 $\Rightarrow \theta \sim 3 \text{ mas}$
- A typical nearby active star:
 - $r = 10\text{-}500 \text{ pc}$
 - $R = 0.5\text{-}10 R_{\text{sol}}$
- \mapsto Not sufficient resolution.



6.2 INTERFEROMETRY

- D increased by combining telescopes.
- Optical interferometry:
 - Eg. CHARA, VLTI, Keck I-II, Large Binocular Telescope
- Note: Interferometry is not direct imaging, it involves inversion.



The VLT Interferometer with ANTU and MELIPAL

ESO PR Photo 30a/01 (5 November 2001)

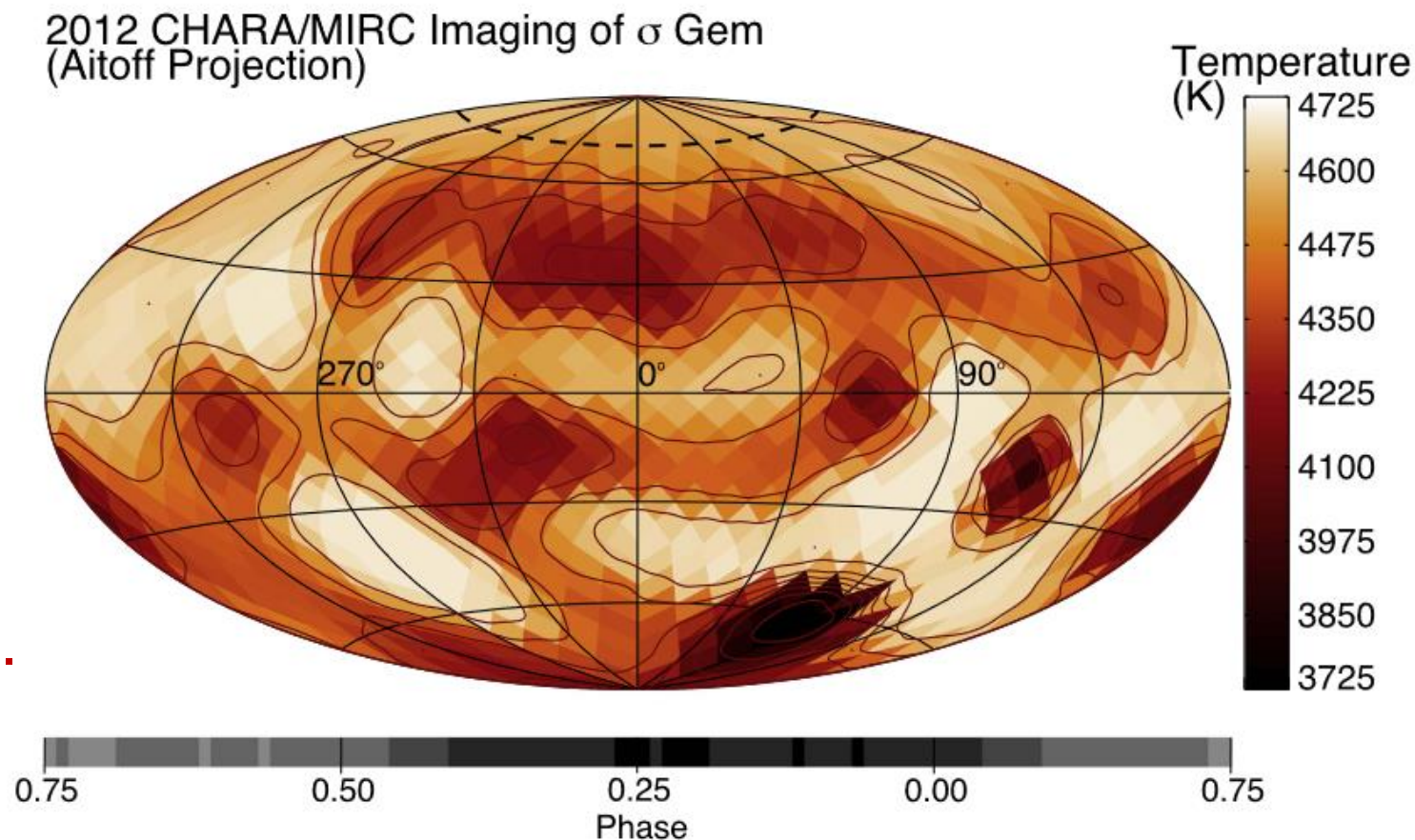
© European Southern Observatory





6.2.1 INTERFEROMETRY OF σ GEM

CHARA/MIRC interferometric image of σ Gem (Roettenbacher et al. 2017).





6.3 INVERSION METHODS

- The star is observed as a point source.
- Rotationally modulated changes in the light are observed due to spots:
 - **Brightness changes \mapsto Photometric light curve.**
 - **Changes in spectral lines \mapsto Periodical deformation of spectral line profiles.**
 - **Changes in spectropolarimetric signal \mapsto Periodical signal in Stokes V or $VQ&U$.**
- The surface, e.g. temperature distribution, is solved by inversion.



6.4 DOPPLER IMAGING

- Rapidly rotating star \mapsto broad spectral lines.
- A spot will influence the part of a spectral line, which wavelength corresponds to the radial velocity of the surface element.
- *Doppler imaging*: Search for the surface distribution which best reproduces the spectral observations.

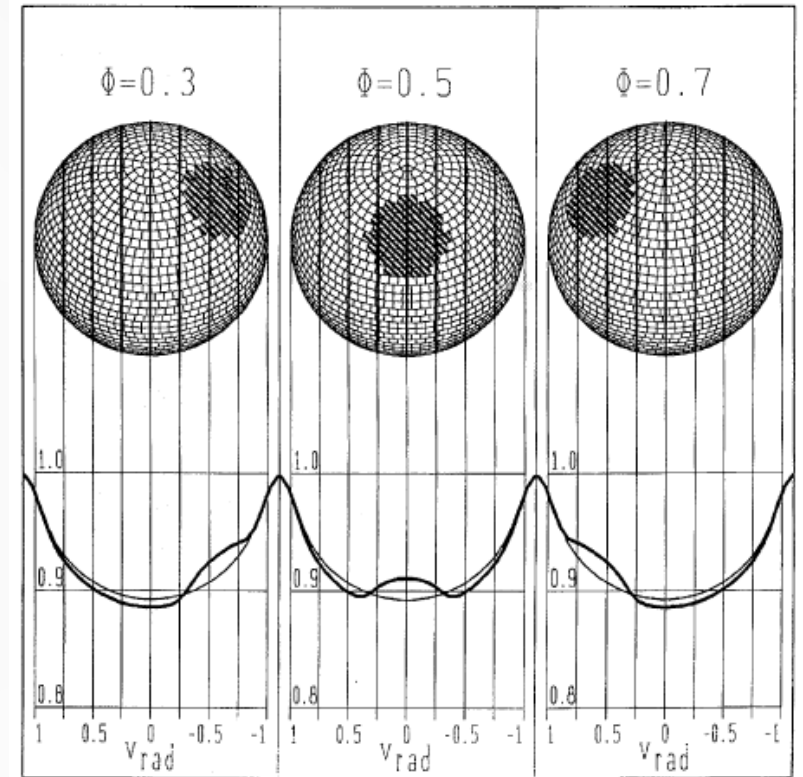


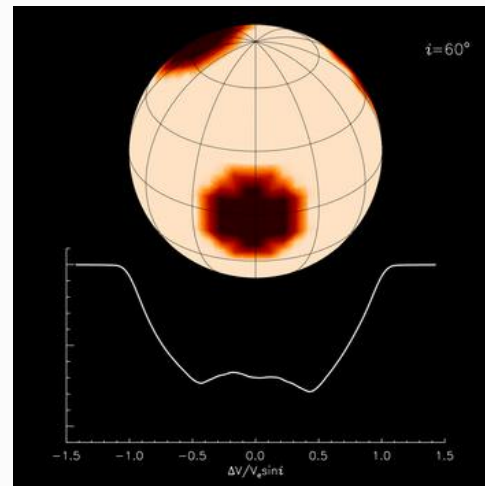
Fig. 2. Absorption line profiles of a spherical non-differentially rotating star with constant local line profile and zero limb-darkening. The spot-to-photosphere brightness ratio is $I_{sp}/I_{ph} = 0.3$; the inclination is $i = 40^\circ$. Shown are three different phases. The observed profiles (heavy lines) are essentially a 1-D projection of the stellar surface. As a comparison, the light lines represent profiles of a spotless star

Kürster, M, 1993, A&A 274, 851



6.4. DOPPLER IMAGING (CONT.)

- Star rotates => spots cause “bumps” moving across the absorption lines.
- Rotational Doppler effect => resolution perpendicular to the projected rotation axis.
- Visibility of the spot => latitudinal resolution.



Animation by O. Kochukhov.

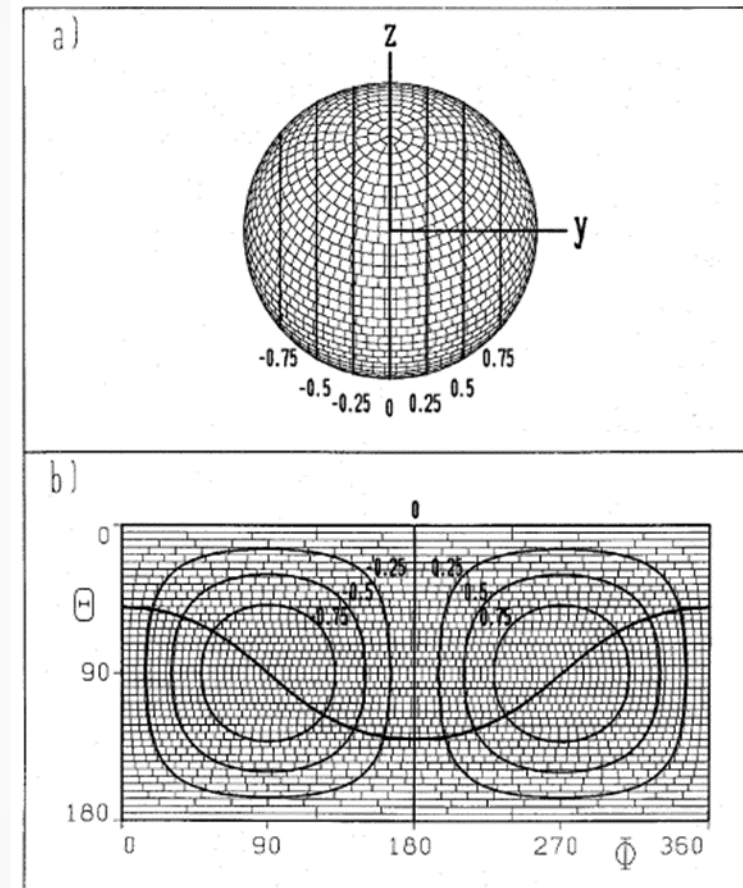


Fig. 1. a and b. Equidistant iso-RV lines on a spherical non-differentially rotating star with inclination $i = 40^\circ$. **a** Projection onto the plane of the sky. **b** Plot of stellar co-latitude θ (90° minus latitude) vs. longitude ϕ . Iso-RV lines are given by Eqs. (10) and (11). At the current rotation phase the area below the heavy cosine line is invisible



6.4.1 FORMULATION OF THE DOPPLER IMAGING PROBLEM

- Search for the solution that minimizes:

$$D(X) = \sum_{\phi_{\text{sp}}, \lambda} \omega_{\phi_{\text{sp}}, \lambda} \frac{(r_{\phi_{\text{sp}}}(\lambda) - r_{\phi_{\text{sp}}}^{\text{obs}}(\lambda))^2}{N_{\phi_{\text{sp}}} N_{\lambda}},$$

where X is the surface distribution of e.g. the temperature and $r_{\phi_{\text{sp}}}$ can be calculated solving radiative transfer in numerical stellar atmosphere.

- D is an operator \Rightarrow solution from D^{-1} .



6.4.2 REGULARISATION

- The problem is ill-posed: The solution is unstable to distortions in the data.
- Solution: An additional constraint:

$$\Phi(X) = D(X) + \Lambda R(X), \quad \text{where } \Lambda \text{ is the } \textit{regularisation} \text{ parameter.}$$

- Different options for the regularisation:

Tikhonov-regularisation (Piskunov et al. 1990): $R(X) = \iint \|\nabla X\|^2 d\sigma,$

Maximum entropy method (Vogt et al. 1987): $R(X) = \iint X \lg X d\sigma$

$d\sigma$ denotes integration over the surface elements.



6.4.3 CALCULATION OF LINE PROFILES

- Errors in $r_{\phi_{\text{sp}}}(\lambda)$ \Rightarrow systematic errors in the image.
- The line profile $r_{\phi_{\text{sp}}}(\lambda)$ is calculated using numerical stellar model atmospheres:
 - Local line profiles are calculated for different values of x and different limb angles on the stellar disk.
 - Using the line profiles table, we can calculate $r_{\phi_{\text{sp}}}(\lambda)$ for a given distribution X .



6.4.3 CALCULATION OF LINE PROFILES

- The stellar flux at wavelength λ :

$$F_{\lambda}(X) = \iint I(x, \lambda + \Delta\lambda) \mu d\sigma,$$

- μ is the cos of the limb angle, $\Delta\lambda$ is the Doppler shift (stellar rotation + radial velocity).
-
- For a realistic profile, F_{λ} is convoluted with
 - macro turbulence and
 - instrumental profile



6.4.3 LINE PROFILES ...

- The integrated line profile is normalised: $r_\lambda = \frac{F_\lambda}{F_{\text{cont}}}$.
- The radiative transfer eq. is solved:

$$I_\lambda(\tau_\lambda) = I_\lambda(0)e^{-\tau_\lambda} + \int_0^{\tau_\lambda} S_\lambda(t_\lambda)e^{-(\tau_\lambda-t_\lambda)} dt_\lambda$$

- The line absorption coefficient: $\kappa_\nu^l = \frac{\pi e^2}{m_e c} f_{ij} N_i g_i \phi(\nu) \frac{e^{-h\nu/kT}}{U(T)} (1 - e^{-h\nu/kT})$
- Continuum absorption:
 - bound-free absorption
 - free-free absorption
 - scattering



6.4.3 CALCULATION OF LINE PROFILES

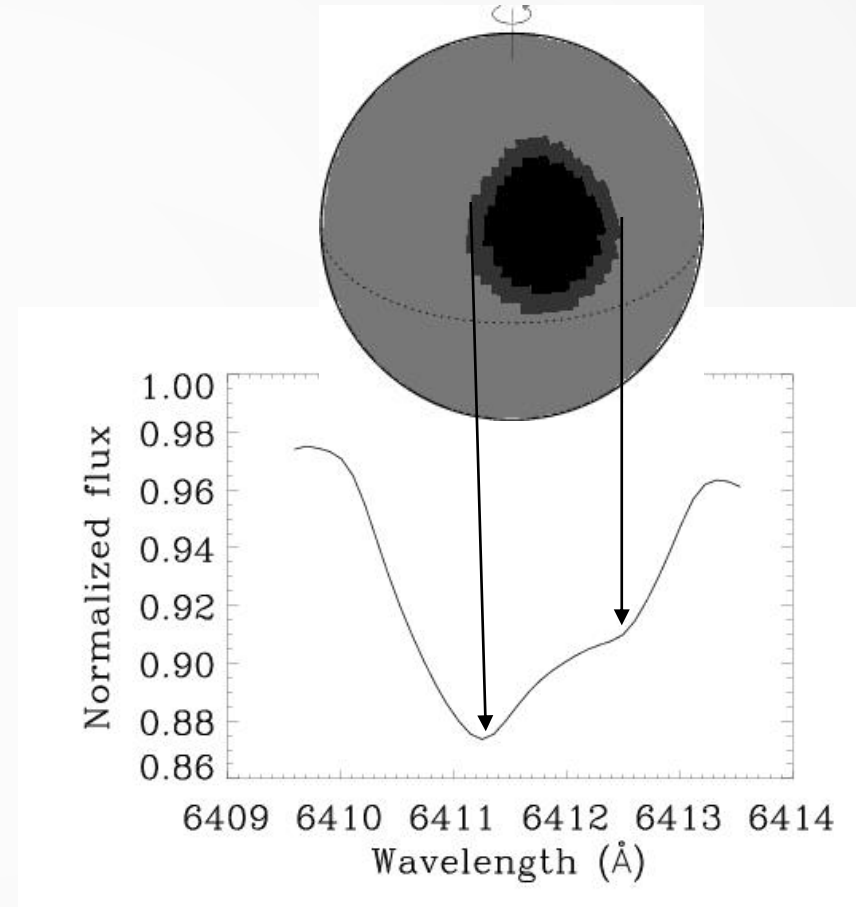
- Spectral broadening mechanisms
 - "Micro level" \mapsto influences the amount of absorption:
 - Radiation damping
 - Collisional broadening
 - Thermal Doppler broadening
 - Micro turbulence
 - Zeeman effect
 - "Macro level" \mapsto no effect on the amount of absorption:
 - Macro turbulence
 - Stellar rotation

Voigt-profile



6.4.4 INTEGRATED LINE PROFILE

- The effect of a spot:
 - Line absorption changes:
 - Typically, absorption is stronger in a cool spot
 - The continuum radiation changes
 - Continuum is weaker in the spot.
 - Continuum usually dominates
↳ *"emission bump"*.





6.4.5 OTHER ADDITIONAL CONSTRAINTS

- Line profiles are calculated from a limited temperature interval $[T_{\min}, T_{\max}]$
- ... but the solution is not necessarily constrained to this interval
- \mapsto can be useful to constraint the solution: $T_{\min} \leq T \leq T_{\max}$
- This can be done with a penalty function



6.4.6 REQUIREMENTS FOR DOPPLER IMAGING ON STELLAR PARAMETERS

- Rapid rotation:
 - The projected rotation velocity much larger than other line broadening.
 - $\mapsto v \sin i > 15 \text{ km/s}$
- An estimate of the resolution along the stellar equator:

$$N_{\text{res}} \sim \frac{4v \sin i}{w_{\text{fwh}}},$$

w_{fwh} is the FWHM of the spectral line without rotation.



6.4.7 OBSERVATIONAL REQUIREMENTS

- High quality spectral observations:
 - At 6400 Å we need resolution $R > 40000$.
 - Signal-to-noise ratio $S/N > 200$.
 - Exposure times shorter than $P_{\text{rot}} / N_{\text{res}}$.
 - At least 10 spectra, evenly distributed over rotation phases.
 - Observation set shorter than timescale of changes in starspot structure.



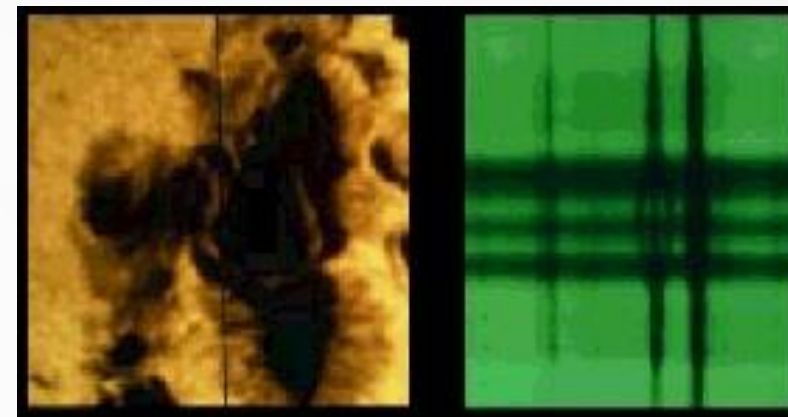
6.4.8 PRACTICAL PROBLEMS

- Rapid rotation and binarity may change the stars geometry.
- Timescale of spot evolution?
- Possible differential rotation.
- Strong spectral lines \mapsto Is the LTE-approximation valid?
- Uncertain parameters \mapsto systematic errors.
- How does the magnetic fields effect the atmosphere?

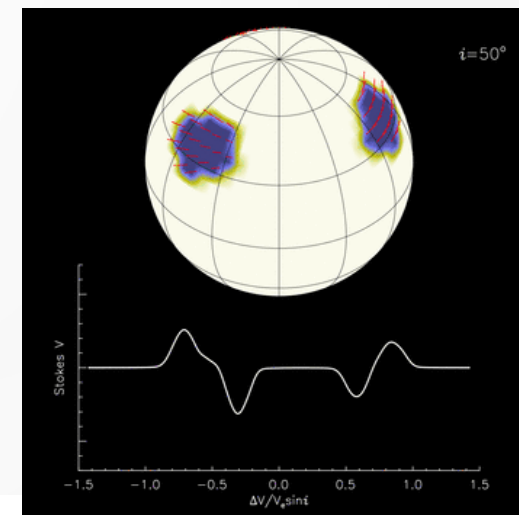


6.5 ZEEMAN-DOPPLER IMAGING (ZDI)

- Magnetic field \mapsto Zeeman effect.
- Z-D –imaging \Rightarrow map the magnetic vector at the stellar surface.
- Spectropolarimetric observations: Stokes parameters $I(\lambda)$, $Q(\lambda)$, $U(\lambda)$, $V(\lambda)$.



Zeeman effect splits lines into separate components.

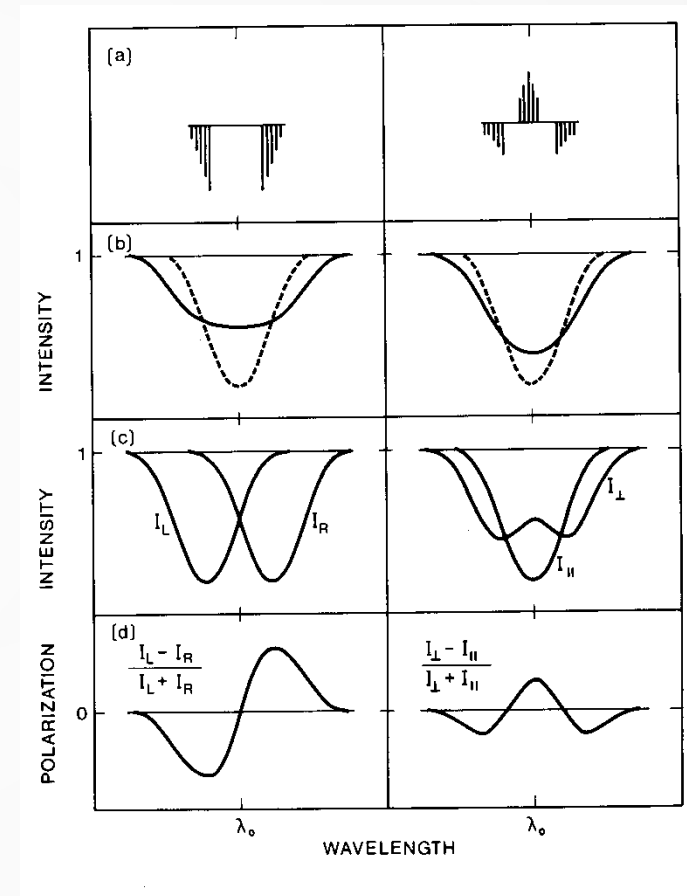


Stokes V-signal of rotating star with magnetic spots (Kochukhov).



6.5.1 INFLUENCE OF MAGNETIC FIELD ON SPECTRAL LINE

- Magnetic field causes polarisation and Zeeman splitting:
 - (a): Zeeman components in longitudinal (left) and transverse (right) field.
 - (b): Observed spectral line intensity profile I without (·····) and with magnetic field (—).
 - (c): Polarisation components: Circular (left panel) and linear polarisation (right panel).
 - (d): Observed Stokes parameters: V (left) and Q or U (right).



Landstreet, 2008, Univ. of Western Ontario, Kanada

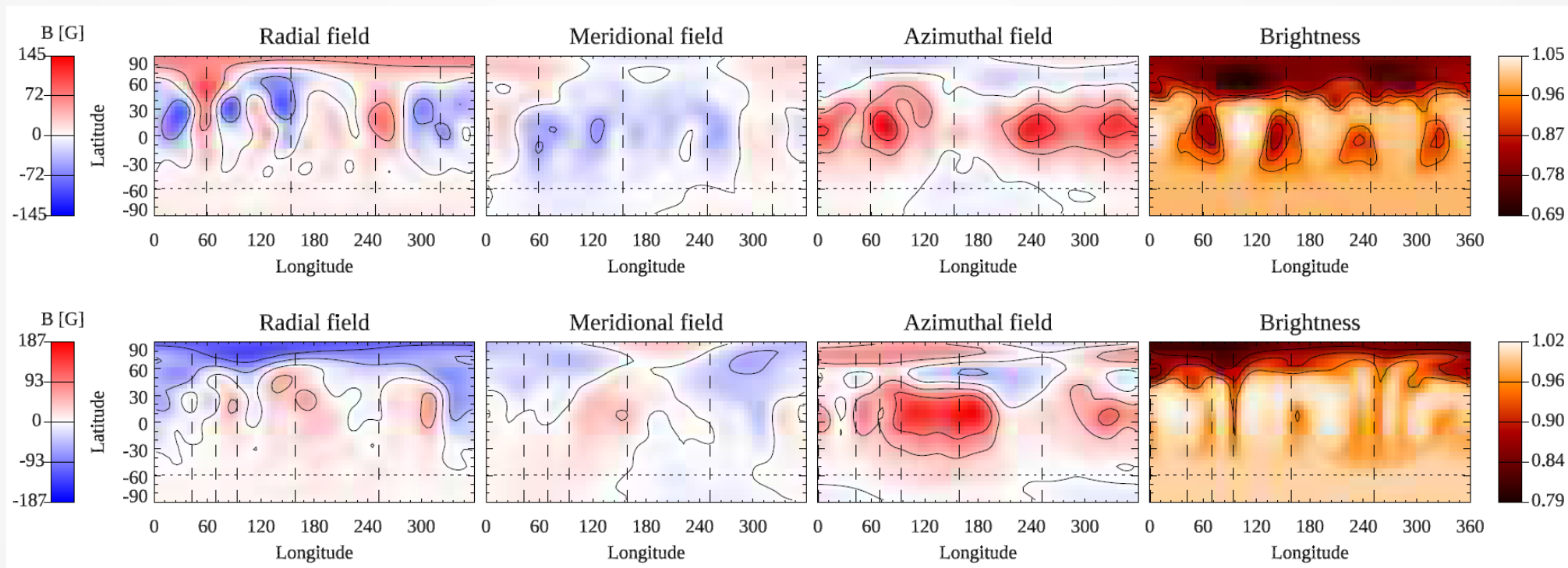


6.5.2 ZDI METHOD

- A further development of Doppler imaging (Semel 1989; Brown et al. 1991; Kochukhov et al. 2014).
- Instead of just intensity spectra ($r_{\phi_{sp}}$), Stokes I&V or full Stokes IVQ&U are used as observations.
- Usually based on spherical harmonics expansion:
 - Easier to employ constraint of source free magnetic field.
 - Easier to derive topology of solution; axisymmetric/non-axisymmetric, poloidal/toroidal field.
- Polarisation signal in single line weak \Rightarrow combination of thousands of lines necessary (e.g., Least Squares Deconvolution, Donati et al. 1997; Kochukhov et al. 2010).



6.5.3 ZDI MAPS OF YOUNG SOLAR ANALOGUE



V1358 Ori, spectral class F9V, $P_{\text{rot}} \approx 1.36\text{d}$, age ~ 30 Myr. ZDI maps from 2013 and 2017 (Willamo et al. 2022).



6.6 EXOPLANETARY TRANSIT MAPPING

- Planetary transits over spots => model of spot size/temperature.

Light curve of HD 209458 with planetary transit (IAA, Deeg & Garrido).
Simulation of Jupiter transiting over the Sun (Haris-Kiss, 2023).

